Frontiers in Health Informatics
ISSN-Online: 2676-7104
www.healthinformaticsjournal.com
2024; Vol 13: Issue 8
Open Access

Green Synthesis Of Selenium And Zinc Oxide Nanoparticles Using *Andrographis Paniculata* And Its Anti-Inflammatory Effect On Hepg2 Cell Line

Yasmin M[1] ,Dr. Mary Agnes A[2*] , Dr. Sindhuja G[3] , Philomina A F[4]

[1]Research Scholar, Department of Zoology, Auxilium College (Autonomous), Affiliated to Thiruvalluvar University, Vellore-622006, TN, India.

[2*]Associate Professor, Department of Zoology, Auxilium College (Autonomous), Affiliated to Thiruvalluvar University, Vellore-622006, TN, India. Email id: agnesanthony14@gmail.com

[3]Assistant Professor, Department of Zoology, Islamiah Women's arts and Science College, Affiliated to Thiruvalluvar University, Vaniyambadi, TN, India.

[4]Research Scholar, Department of Zoology, Auxilium College (Autonomous), Affiliated to Thiruvalluvar University, Vellore-622006, TN, India.

Cite this paper as: Yasmin M, Dr. Mary Agnes A, Dr. Sindhuja G, Philomina A F (2024) Green Synthesis Of Selenium And Zinc Oxide Nanoparticles Using Andrographis Paniculata And Its Anti-Inflammatory Effect On Hepg2 Cell Line". *Frontiers in Health Informatics,* (8), 5641-5661

ABSTRACT

The present study focuses on the green synthesis of selenium and zinc oxide nanoparticles using *Andrographis paniculata*, a medicinal plant known for its rich phytochemical content. The plant extract served as a natural reducing and stabilizing agent, enabling an eco-friendly synthesis approach. Characterization of the synthesized nanoparticles confirmed their stability and the presence of functional groups responsible for bioreduction, as revealed by FTIR analysis. The cytotoxicity of the nanoparticles was evaluated using the MTT assay on HepG2 cells, revealing a dose-dependent response. Notably, lower concentrations (1–10 µg/ml) exhibited reduced toxicity, indicating their potential biocompatibility. Furthermore, the anti-inflammatory activity of the nanoparticles was assessed using the albumin denaturation assay, demonstrating significant inhibition, especially at lower doses. These findings suggest that selenium and zinc oxide nanoparticles synthesized via *Andrographis paniculata* possess promising anti-inflammatory properties and may serve as potential candidates for therapeutic applications with minimal cytotoxic effects.

Keywords: Green synthesis, Selenium nanoparticles, Zinc oxide nanoparticles, *Andrographis paniculata*, HepG2 cells, Anti-inflammatory activity, Cytotoxicity.

INTRODUCTION

Nanotechnology is an emerging interdisciplinary field involving the fabrication, manipulation, and application of materials at the nanoscale range (1–100 nm). Nanomaterials exhibit unique physicochemical properties such as high surface-to-volume ratio, enhanced strength, improved stability, and biocompatibility. These properties make them promising candidates for biomedical

applications including drug delivery, diagnostics, and therapeutics (S. Mehnath *et al.,* 2021).

Since the late 1980s, research has progressed toward second-generation drug delivery systems, focusing on green nanomaterial synthesis combined with conventional drug delivery strategies (Keservani R.K. et al., 2018). A successful drug delivery system should exhibit high drug loading capacity, prolonged circulation time, protection of therapeutic agents from degradation, targeted delivery, controlled and sustained release, and compatibility with various routes of administration (Park, K., 2014).

Green Synthesis Method

Green synthesis is an eco-friendly approach that utilizes plant extracts for the bioreduction of metal ions into nanoparticles. This method is simple, cost-effective, non-toxic, and sustainable. The phytochemicals present in plant extracts—such as flavonoids, terpenoids, alkaloids, and phenolic compounds—serve as reducing and stabilizing agents during nanoparticle formation (Hussain I. et al., 2016; Kharissova O.V. et al., 2013).

Using water as a reducing solvent further enhances the green credentials of this method. It provides benefits such as scalability, medicinal compatibility, and environmental safety. Plant-derived nanoparticles have shown great potential in biomedicine and environmental applications (Noruzi, 2015; Singh P. et al., 2016).

Andrographis Paniculata

Andrographis paniculata, also known as green chiretta or creat, is a well-known medicinal plant belonging to the Acanthaceae family. It is native to India and Sri Lanka and is widely used across Asia in traditional medicine to treat bacterial and viral infections ("Traded Medicinal Plants Database").

Phytochemical studies have identified labdane diterpenoid lactones, flavonoids, and various other bioactive compounds in *A. paniculata*. These constituents are responsible for its wide range of pharmacological activities, including antimicrobial, cytotoxic, antioxidant, anti-inflammatory, hepatoprotective, antidiabetic, and immunomodulatory properties (Mishra S.K. et al., 2007; & Chandrasekaran C.V. et al., 2010).

Due to its therapeutic potential and rich phytochemical profile, *A. paniculata* has gained attention for the green synthesis of nanoparticles intended for biomedical applications.

Selenium Nanoparticles

Selenium (Se) is a metalloid and an essential trace element required for human health. It plays a critical role in antioxidant defense, immune function, and thyroid hormone metabolism. Recent studies have demonstrated its anticancer potential, particularly in reducing the risk of lung and prostate cancers (Tran & Webster, 2011). Selenium-enriched probiotics have also been found to inhibit pathogenic microorganisms.

Selenium nanoparticles (SeNPs) have gained significant attention due to their enhanced bioavailability and multifunctional properties. These include antioxidant activity, anticancer potential, antimicrobial effects, anti-inflammatory activity, imaging capabilities, and suitability for drug delivery applications—all while maintaining low toxicity.

Zinc oxide Nanoparticles

Zinc oxide nanoparticles (ZnO NPs) are among the most widely used metal oxide nanoparticles due to their unique optical, chemical, and biological properties (W.C.W. Chan et al., 2010). These nanoparticles exhibit high surface area, semiconducting behaviour, photocatalytic activity, and the ability to generate reactive oxygen species (ROS), which contribute to their antimicrobial and anticancer properties.

ZnO NPs have demonstrated strong antibacterial, anti-inflammatory, antioxidant, and wound-healing properties, making them potential candidates for treating infections, inflammation, and tissue regeneration (E.Z. Gomaa, 2022). Their ability to interact with biomolecules also supports their use in biosensors and diagnostic tools.

HepG2 Cell Line and Its Relevance in Anti-Inflammatory Research

HepG2 is a widely used immortal human liver cancer cell line, originally derived from a 15-year-old male with hepatocellular carcinoma (Aden, D. P., et al., 1979). Despite being a cancer cell line, HepG2 retains many important functions of normal liver cells, including the production of plasma proteins, metabolic enzymes, and transport proteins. This makes it an ideal in vitro model for studying liver metabolism, hepatotoxicity, drug screening, and disease mechanisms. In toxicological studies, HepG2 cells are routinely used to assess the cytotoxic effects of pharmaceutical compounds and nanoparticles, thereby aiding in the development of safer drugs.

Nanoparticles and their Anti-Inflammatory Potential

Nanoparticles (NPs), owing to their small size and high surface area-to-volume ratio, exhibit significant anti-inflammatory properties. This enhanced surface reactivity improves their interaction with biological membranes and inflammatory mediators. One of the key mechanisms by which NPs exert anti-inflammatory effects is by scavenging reactive oxygen species (ROS), which are central to oxidative stress and inflammation.

As a result, nanoparticles have emerged as promising candidates for the treatment and management of inflammation-related diseases, including liver inflammation.

MATERIALS AND METHODS

Preparation of *Andrographis paniculata* Leaf Extract

Fresh leaves of *Andrographis paniculata* were collected, thoroughly washed with running tap water, and rinsed with distilled water to remove any surface impurities. The cleaned leaves were finely chopped and boiled in distilled water for a short duration. After boiling, the mixture was allowed to cool and then filtered using Whatman filter paper. The filtrate was used freshly within one hour for nanoparticle synthesis.

Preparation of Selenous Acid Solution

Selenous acid was dissolved in distilled water and stirred using a magnetic stirrer until a clear solution was obtained. This served as the precursor solution for selenium nanoparticle synthesis.

Synthesis of Selenium Nanoparticles

Freshly prepared *Andrographis paniculata* extract was added to the selenous acid solution. The mixture was heated using a water bath for a specific period. Ascorbic acid was then added as a reducing agent, which led to a visible color change, indicating the formation of selenium nanoparticles. The solution was allowed to settle, and the supernatant was discarded. The resulting nanoparticles were collected, dried, and stored for further analysis.

Synthesis of Zinc Oxide Nanoparticles

The synthesis procedure for zinc oxide nanoparticles was similar to that of selenium nanoparticles, with the exception that ascorbic acid was not added. The plant extract was mixed with the zinc precursor solution and heated. After completion of the reaction, the nanoparticles were collected, dried, and scrapped for further characterization.

RESULT AND DISCUSSION

Characterization of Selenium and Zinc oxide Nanoparticles synthesized using *Andrographis paniculata* (Se-Ap)

Field Emission Scanning Electron Microscopy (FESEM) Analysis - for Morphological identification.

Fourier Transform Infra-Red Spectroscopy (FTIR) for functional group identification.

X-Ray Diffraction (XRD) for crystalline structure analysis.

FESEM analysis of Selenium-*Andrographis paniculata* (Se-Ap)

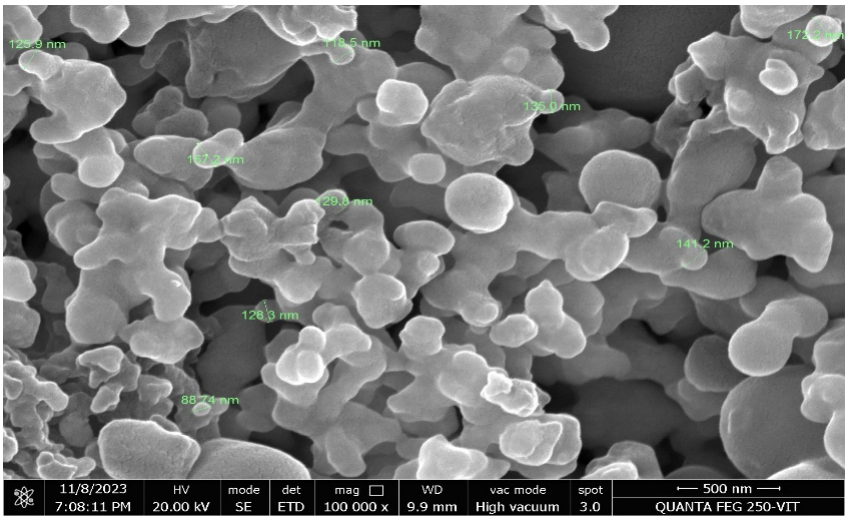

Figure 1: FESEM images of SeNPs synthesized using *Andrographis paniculata*

The FESEM images reveal that the selenium nanoparticles synthesized using *Andrographis paniculata* possess a predominantly spherical morphology. The particles are moderately dispersed with slight agglomeration, which is commonly observed in biogenically synthesized nanoparticles. The size of the nanoparticles ranges approximately between 50 to 100 nm. The spherical structure and nanoscale dimensions confirm successful nanoparticle synthesis via a green route. The agglomeration observed might be due to the natural phytochemical capping agents from the plant extract, which help in

stabilization but may also cause slight clustering.

XRD analysis of Selenium-*Andrographis paniculata* (Se-Ap)

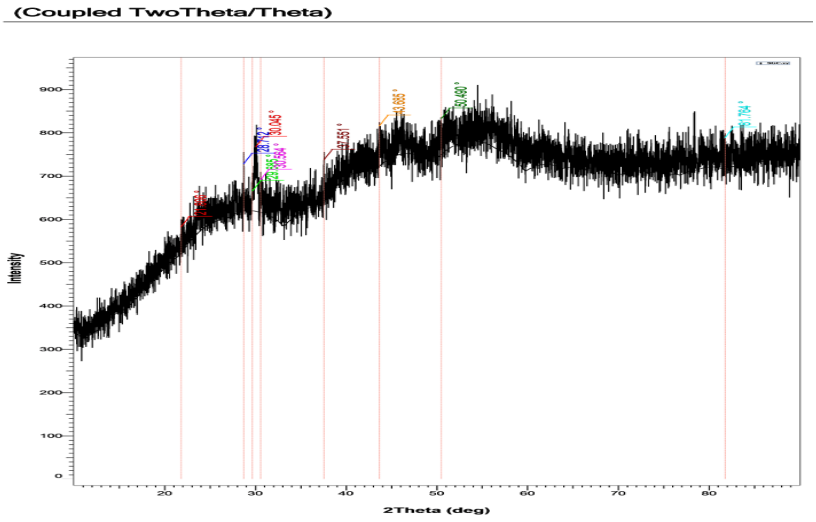

Figure 2: XRD pattern of SeNPs synthesized using *Andrographis paniculata*

The XRD pattern of Se-Ap nanoparticles displays distinct peaks at 2θ values of 27.685°, 28.737°, 30.045°, 42.551°, 43.865°, 50.490°, and 61.764°, indicating the crystalline nature of the synthesized nanoparticles. The prominent peak at 28.737° is particularly noteworthy, as it corresponds to the characteristic reflection of elemental selenium. The presence of multiple diffraction peaks suggests a polycrystalline structure. These results confirm that the synthesized selenium nanoparticles exhibit good crystallinity and are in alignment with the standard diffraction data for selenium.

FTIR analysis of Selenium-*Andrographis paniculata* (Se-Ap)

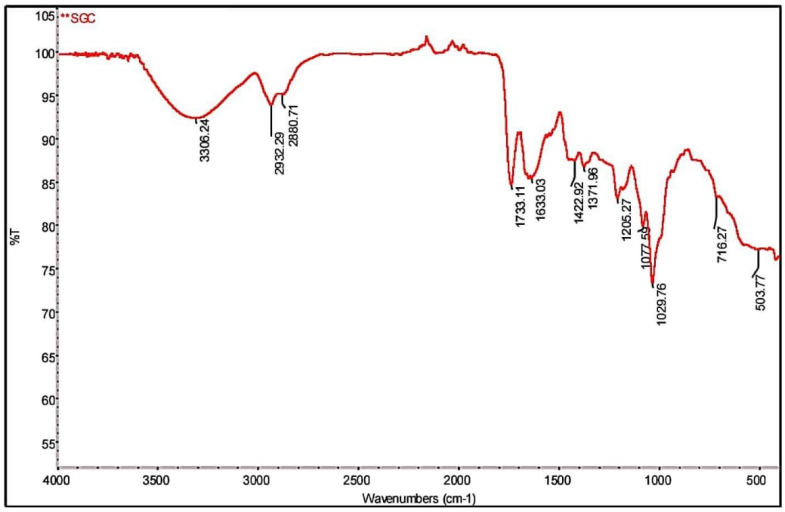

Figure 3: FTIR spectrum of SeNPs synthesized using *Andrographis paniculata*

The FTIR spectrum confirms the involvement of various phytochemicals from *Andrographis paniculata* in the synthesis of selenium nanoparticles. Key peaks indicate the presence of hydroxyl

(O–H), alkane (C–H), ester/carboxylic acid (C=O), aromatic or amide (C=C), and alcohol/ether (C–O) groups. Peaks related to C–N stretching and metal–oxygen bonds further support the reduction and stabilization process. These findings highlight the role of flavonoids, phenolics, and proteins in the bioreduction and stabilization of selenium nanoparticles.

Characterization of Zinc Nanoparticles Synthesized Using *Andrographis paniculata*

FESEM analysis *Andrographis paniculata* (Zn-Ap)

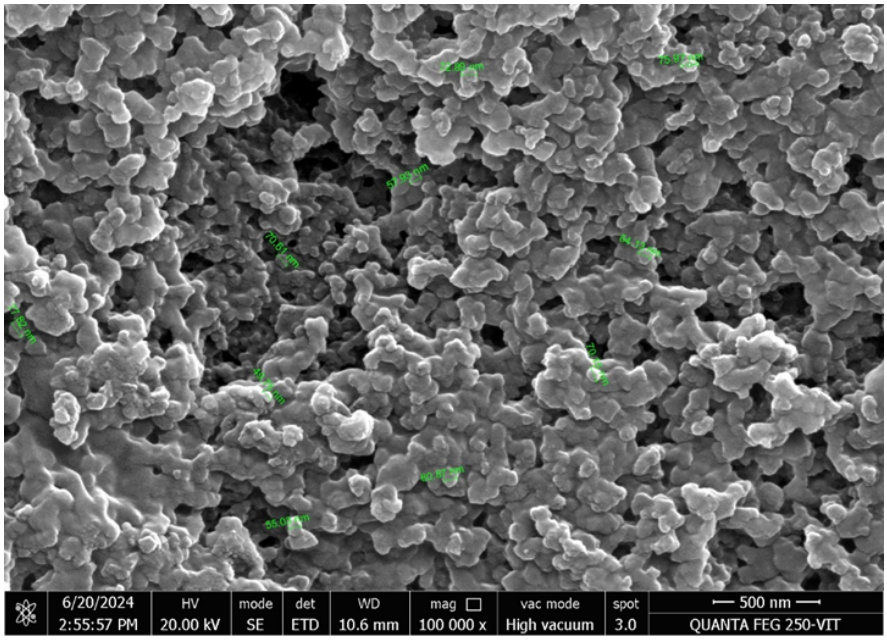

Figure 4: FESEM image of ZnO NPs synthesized using *Andrographis paniculata*.

The Field Emission Scanning Electron Microscopy (FESEM) analysis of Zn-Ap nanoparticles revealed a particle size range from 49.76 nm to 77.82 nm. The measured sizes include 55.03 nm, 49.76 nm, 64.13 nm, 70.15 nm, 60.87 nm, 75.97 nm, 72.89 nm, 70.61 nm, and 77.82 nm. This indicates a moderate variation in size, with most particles falling between 49.76 nm and 75.97 nm. The relatively uniform size distribution suggests that the synthesized nanoparticles are fairly consistent in morphology. This consistency makes Zn-Ap nanoparticles suitable for applications such as drug delivery, catalysis, and environmental remediation, where medium-sized nanoparticles are often preferred.

XRD analysis of Zinc - *Andrographis paniculata* (Zn-Ap)

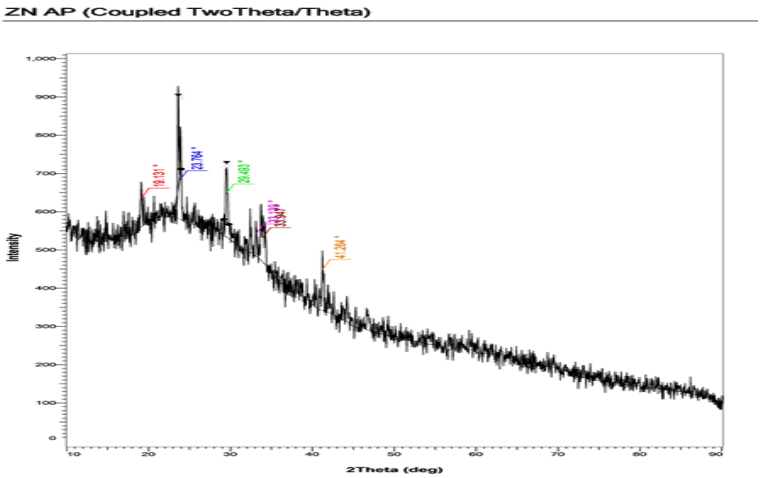

Figure 5: XRD pattern of ZnO NPs synthesized using *Andrographis paniculata*.

The X-ray diffraction (XRD) analysis of Zn-Ap nanoparticles reveals key diffraction peaks at 19.131°, 23.764°, 29.493°, 33.479°, and 41.264° (2θ). These peaks are indicative of the crystalline nature of the synthesized nanoparticles and suggest the presence of both zinc (Zn) and zinc oxide (ZnO) phases. The sharp and well-defined peaks reflect good crystallinity, while broader peaks may suggest the presence of nanoscale crystallites or a minor amorphous phase. These results confirm the successful formation of ZnO nanoparticles through a green synthesis approach.

FTIR analysis Zinc - *Andrographis paniculata* (Zn-Ap)

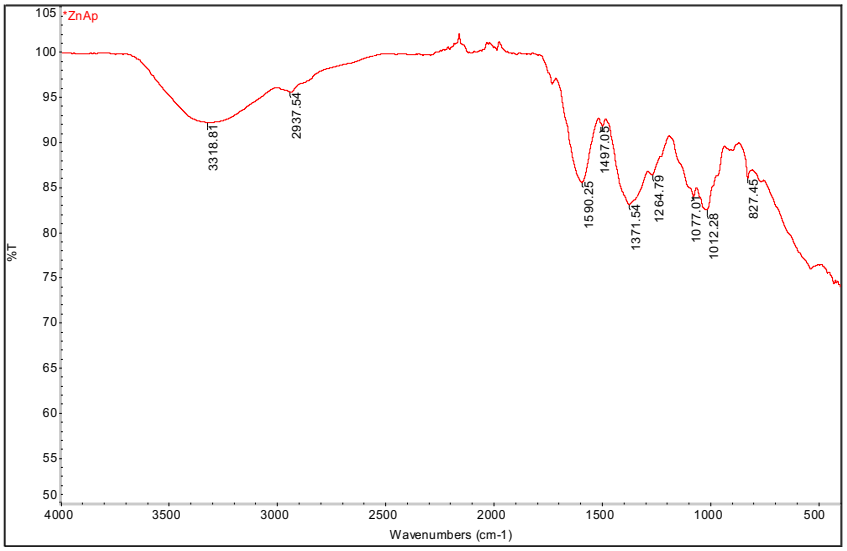

Figure 6: FTIR spectrum of ZnO NPs synthesized using *Andrographis paniculata*.

The FTIR spectrum of Zn-Ap nanoparticles indicates the presence of key functional groups from *Andrographis paniculata* involved in nanoparticle synthesis. Peaks corresponding to O–H, C–H, C=C, N–O, C–O/C–N, and aromatic C–H vibrations suggest the presence of phenolics, flavonoids, nitro compounds, and glycosides. These phytochemicals act as reducing and stabilizing agents, confirming

their essential role in the green synthesis of zinc oxide nanoparticles.

MTT Result of Selenium – *Andrographis paniculata* (Green chiretta) (Se-Gc)

The Selenium – *Andrographis paniculata* (Se-Gc) was tested for *in vitro* cytotoxicity, using Hep-G2 cells by MTT assay. The OD value are as follows

Table 1: OD Value at 570 nm of Selenium - *Andrographis paniculata* (Se-Gc)

S. No.	Tested sample concentration (µg/ml)	OD value at 570 nm (in triplicates)			Mean OD Value
1	Control	0.407	0.415	0.418	0.418
2	500 µg/ml	0.123	0.127	0.125	0.125
3	400 µg/ml	0.137	0.142	0.139	0.139
4	300 µg/ml	0.198	0.189	0.193	0.193
5	200 µg/ml	0.199	0.196	0.197	0.197
6	100 µg/ml	0.207	0.211	0.209	0.209
7	50 µg/ml	0.219	0.223	0.221	0.221
8	25 µg/ml	0.279	0.286	0.282	0.282
9	10 µg/ml	0.299	0.301	0.300	0.300
10	5 µg/ml	0.301	0.312	0.306	0.306
11	1 µg/ml	0.357	0.342	0.349	0.349

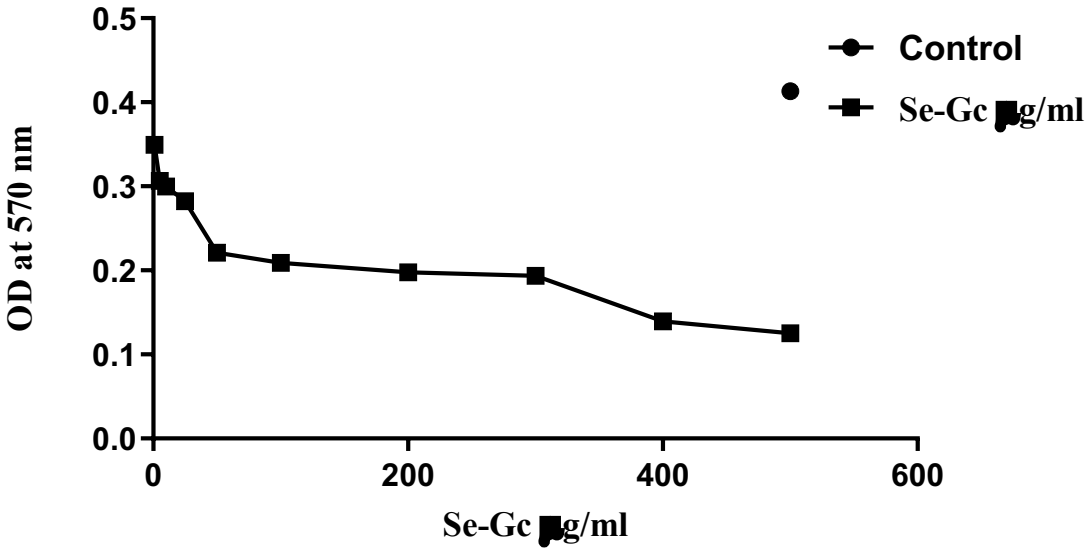

Figure 7: Line graph of Se-Gc

The optical density (OD) values at 570 nm for HepG2 cells treated with different concentrations of Se-Gc nanoparticles, as measured by the MTT assay, indicate a dose-dependent cytotoxic effect. The control group (untreated cells) exhibits the highest OD value (~0.415), corresponding to 100% cell viability. As the concentration of Se-Gc increases, OD values gradually decrease, demonstrating reduced cell viability. The lowest OD value (~0.125) is observed at 500 µg/ml, indicating significant cytotoxicity at higher concentrations. However, lower concentrations (1–10 µg/ml) (Table 1) exhibit relatively higher OD values compared to higher doses, suggesting reduced toxicity and potential suitability for biological applications at these levels.

Table 2: Cell Viability (%) of Se-Gc

S. No.	Tested sample concentration (µg/ml)	Cell viability (%) (in triplicates)			Mean Value (%)
1	Control	100	100	100	100
2	500 µg/ml	29.758	30.725	30.241	30.241
3	400 µg/ml	33.145	34.354	33.75	33.75
4	300 µg/ml	47.903	45.725	46.814	46.814
5	200 µg/ml	48.145	47.419	47.783	47.782
6	100 µg/ml	50.080	51.048	50.564	50.564
7	50 µg/ml	52.983	53.951	53.467	53.467
8	25 µg/ml	67.5	69.193	68.346	68.346
9	10 µg/ml	72.338	72.822	72.580	72.580
10	5 µg/ml	72.822	75.483	74.153	74.153
11	1 µg/ml	86.371	82.741	84.556	84.556

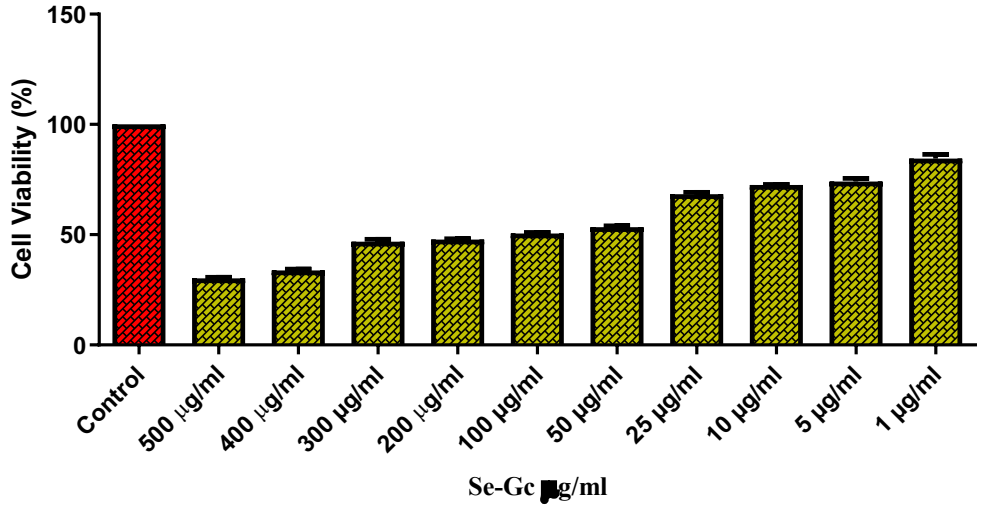

Figure 8:

Bar graph showing HepG2 cell viability (%) of Se-Gc

The cell viability of HepG2 cells treated with different concentrations of Se-Gc nanoparticles was assessed using the MTT assay (Table 2). The control group exhibited 100% viability, as expected, while increasing concentrations of Se-Gc nanoparticles led to a dose-dependent decrease in cell viability. The lowest viability (30.241%) was observed at the highest concentration (500 µg/ml), indicating significant cytotoxicity. As the concentration decreased, cell viability gradually increased, reaching 84.556% at 1 µg/ml. Notably, at lower concentrations (1–10 µg/ml), cell viability remained above 70%, and the Bar graph suggest the same, suggesting reduced cytotoxicity and potential for biological applications at these levels (Figure 8).

Table 3: IC50 Value of *Andrographis paniculata* (49.72 µg/ml)

log(inhibitor) vs. normalized response -- Variable slope	
Best-fit values	
LogIC50	1.697
HillSlope	-0.8221
IC50	49.72
95% CI (profile likelihood)	
LogIC50	1.598 to 1.791
HillSlope	-0.9717 to -0.6964
IC50	39.66 to 61.79
Goodness of Fit	
Degrees of Freedom	28
R squared	0.9374
Sum of Squares	1861

Sy.x	8.152
Number of points	
# of X values	30
# Y values analyzed	30

The IC50 value of selenium nanoparticles synthesized using *Andrographis paniculata* (Se-Ap) was determined to be 49.72 µg/ml (Table 3). These findings suggest that Se-Ap nanoparticles exhibit cytotoxic activity against HepG2 cells, warranting further exploration for potential biomedical applications.

MTT Result of Zinc – *Andrographis paniculata* (Green Chiretta) (Zn-Gc)

The Zn-Gc nanoparticles were evaluated for their in vitro cytotoxicity using the MTT assay on HepG2 cells

Table 4: OD Value at 570 nm of Zinc – *Andrographis paniculata* (Zn-Gc)

S. No.	Tested sample concentration (µg/ml)	OD value at 570 nm (in triplicates)			Mean OD Value
1	Control	0.435	0.48	0.457	0.457
2	500 µg/ml	0.142	0.15	0.146	0.146
3	400 µg/ml	0.149	0.148	0.148	0.148
4	300 µg/ml	0.157	0.169	0.163	0.163
5	200 µg/ml	0.160	0.170	0.165	0.165
6	100 µg/ml	0.183	0.198	0.190	0.190
7	50 µg/ml	0.199	0.188	0.193	0.193
8	25 µg/ml	0.191	0.209	0.200	0.200
9	10 µg/ml	0.203	0.198	0.200	0.200
10	5 µg/ml	0.226	0.205	0.215	0.215
11	1 µg/ml	0.225	0.214	0.219	0.219

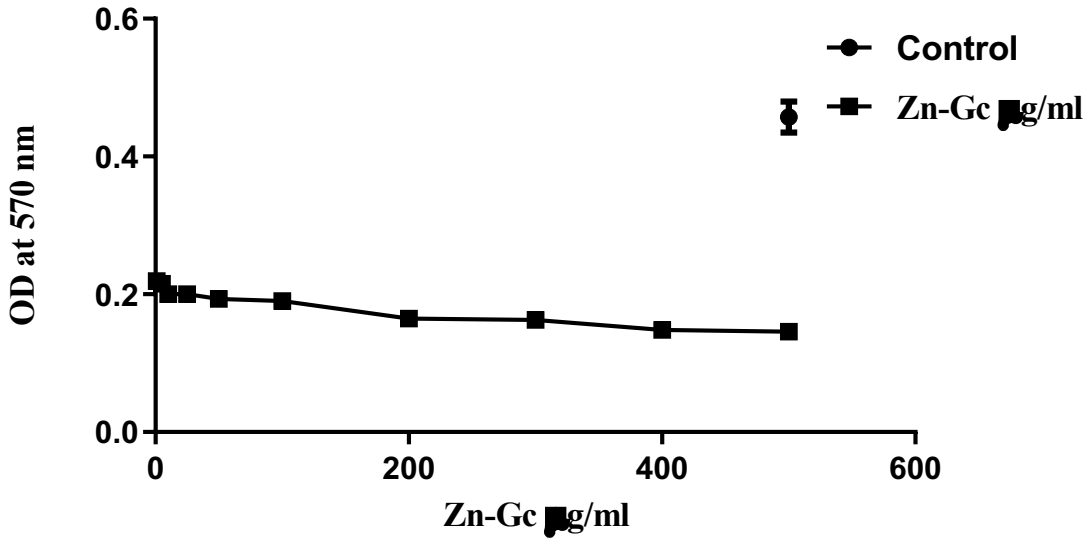

Figure 9: Line graph of Zn-Gc

The OD values at 570 nm for Zn-Gc nanoparticles treated HepG2 cells were recorded across different concentrations to determine cytotoxicity using the MTT assay. The control group exhibited the highest OD values, indicating maximum cell viability. A progressive decline in OD values was observed with increasing Zn-Gc concentrations, suggesting a dose-dependent cytotoxic effect. The lowest OD value was recorded at 500 µg/ml, indicating significant cell death. At lower concentrations (10–1 µg/ml), the OD values remained relatively stable, suggesting reduced cytotoxicity and potential biocompatibility at these levels.

Table 5: Cell Viability (%) of Zn-Gc

S. No.	Tested sample concentration (µg/ml)	Cell viability (%) (in triplicates)			Mean Value (%)
1	Control	100	100	100	100
2	500 µg/ml	31.038	32.786	31.912	31.912
3	400 µg/ml	32.568	32.349	32.459	32.459
4	300 µg/ml	34.316	36.939	35.628	35.628
5	200 µg/ml	34.972	37.158	36.065	36.065
6	100 µg/ml	40	43.278	41.639	41.639
7	50 µg/ml	43.497	41.092	42.295	42.295
8	25 µg/ml	41.748	45.683	43.715	43.715
9	10 µg/ml	44.371	43.278	43.825	43.825
10	5 µg/ml	49.398	44.808	47.103	47.103

11	1 µg/ml	49.180	46.776	47.978	47.978

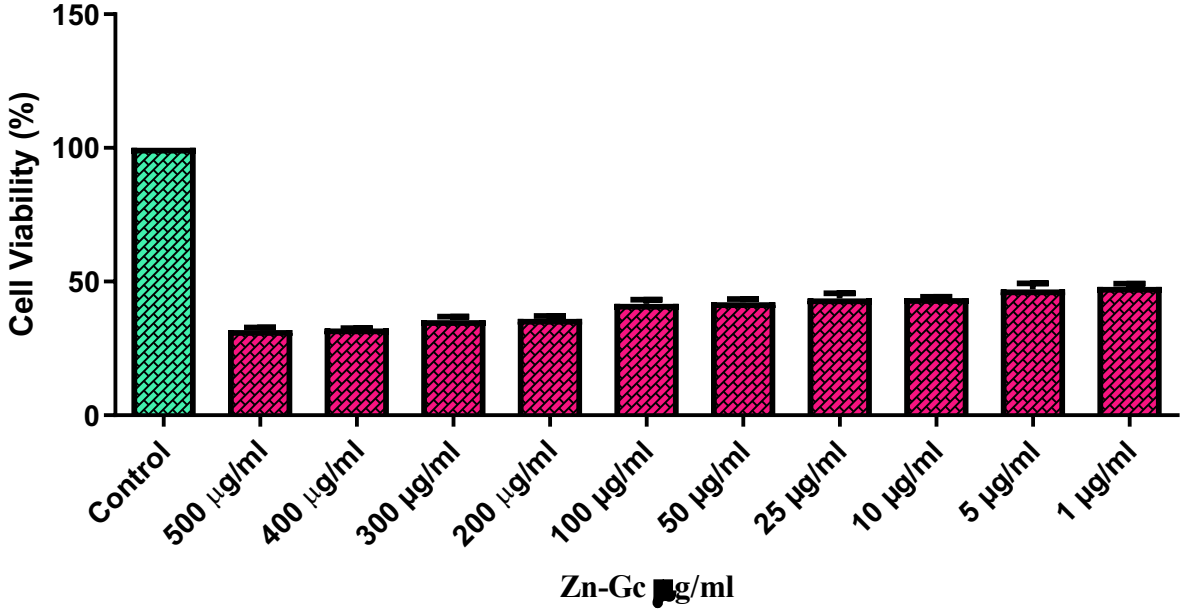

Figure 10: Bar graph showing HepG2 cell viability (%) of Zn-Gc

The cell viability of HepG2 cells treated with Zn-Gc nanoparticles was assessed using the MTT assay. The control group exhibited 100% viability, while a dose-dependent reduction in viability was observed with increasing concentrations of Zn-Gc. At 500 µg/ml, the lowest cell viability (31.91%) was recorded, indicating significant cytotoxicity. However, at lower concentrations (10–1 µg/ml), the cell viability remained relatively higher, suggesting reduced cytotoxicity and potential biocompatibility. The bar graph visually represents the trend, highlighting the inverse relationship between Zn-Gc concentration and cell viability (Table 5).

Table 6: IC50 Value of Zinc – *Andrographis paniculata* (77.41 µg/ml)

log(inhibitor) vs. normalized response	
Best-fit values	
LogIC50	1.889
IC50	77.41
95% CI (profile likelihood)	
LogIC50	1.770 to 2.004
IC50	58.88 to 100.8
Goodness of Fit	
Degrees of Freedom	29
R squared	0.8906
Sum of Squares	4060

Sy.x	11.83
Number of points	
# of X values	30
# Y values analyzed	30

The IC50 value of zinc nanoparticles synthesized using *Andrographis paniculata* (Zn-Ap) was determined to be 77.41 µg/ml (Table 6), indicating the concentration required to inhibit 50% of HepG2 cell viability. These findings suggest that Zn-Ap nanoparticles exhibit cytotoxic activity against HepG2 cells, though with a relatively higher IC50 value, indicating lower potency compared to more cytotoxic nanoparticles. The absorbance for each well was measured at 570 nm using a microplate reader (Thermo Fisher Scientific, USA) and the percentage cell viability and IC50 value were calculated using Graph Pad Prism 6.0 software (USA).

Anti-inflammatory activity of Selenium – *Andrographis paniculata*

The anti-inflammatory activity of selenium nanoparticles synthesized using *Andrographis paniculata* (Se-Gc) was evaluated through the albumin denaturation assay.

Table 7: OD Value at 660 nm of Selenium – *Andrographis paniculata* (Se-Gc)

S. No	Tested sample concentration (µg/ml)	OD Value at 660 nm (in triplicates)			Mean OD Value
1.	Control	1.778	1.798	1.829	1.802
2.	500 µg/ml	1.123	1.124	1.217	1.155
3.	250 µg/ml	1.218	1.252	1.253	1.241
4.	100 µg/ml	1.256	1.257	1.271	1.261
5.	50 µg/ml	1.272	1.285	1.314	1.290
6.	10 µg/ml	1.474	1.465	1.474	1.471
7.	Standard	1.109	1.056	1.078	1.081

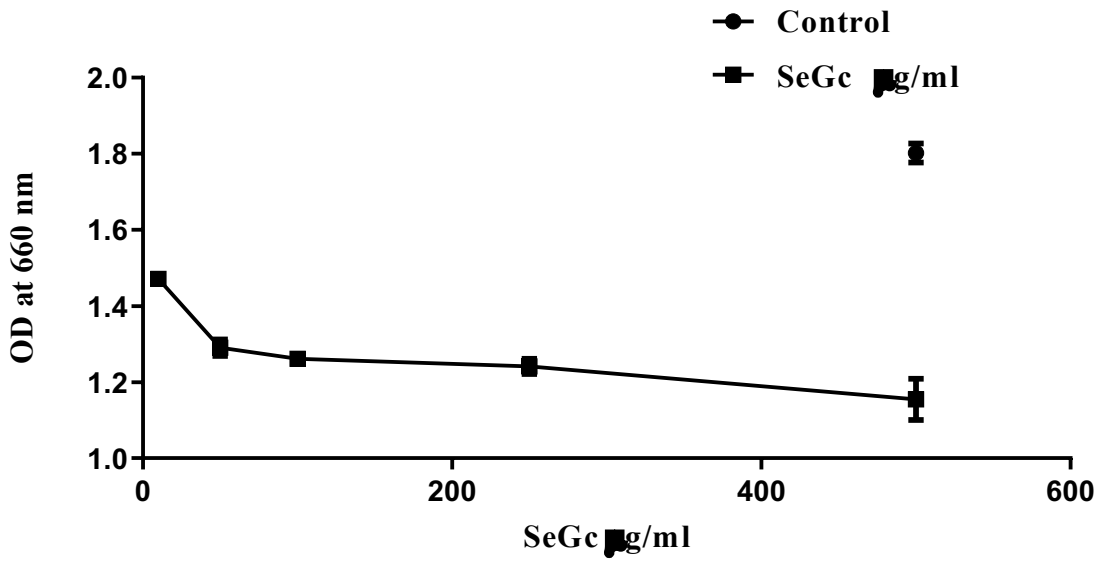

Figure 11: Line graph of Se-Gc

The optical density (OD) values at 660 nm indicate the extent of protein denaturation, where higher OD values reflect greater denaturation, and lower OD values suggest inhibition of denaturation, signifying anti-inflammatory activity. The control OD (1.802) represents 100% protein denaturation, indicating no inhibition. The standard OD values (1.056–1.109) demonstrate strong inhibition of protein denaturation by the reference anti-inflammatory drug. The test sample, selenium nanoparticles synthesized using *Andrographis paniculata* (Se-Gc), exhibited a concentration-dependent decrease in OD values, indicating higher inhibition at increased concentrations. At 500 µg/ml, the OD values (1.123–1.217) were significantly lower than the control, suggesting notable inhibition of albumin denaturation. As the concentration decreased, the OD values gradually increased (10–250 µg/ml), demonstrating a dose-dependent inhibition effect (Table 7). The OD values at the highest concentration were close to the standard, highlighting the strong anti-inflammatory potential of Se-Gc nanoparticles.

Table 8: Inhibition percentage of albumin denaturation (%) of Se-Gc

S. No	Tested sample concentration (µg/ml)	Inhibition percentage albumin denaturation (%) (in triplicates)			Mean Value (%)
1.	500 µg/ml	37.6804	37.6249	32.4639	35.923
2.	250 µg/ml	32.4084	30.5216	30.4661	31.1321
3.	100 µg/ml	30.2997	30.2442	29.4673	30.0037

4.	50 µg/ml	29.4118	28.6903	27.081	28.3944
5.	10 µg/ml	18.202	18.7014	18.202	18.3685
6.	Standard	38.4573	41.3984	40.1776	40.0111

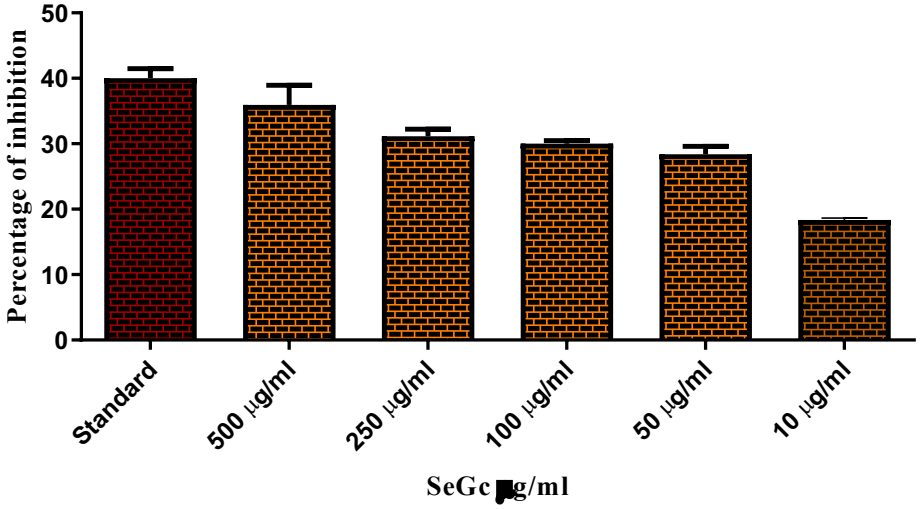

Figure 12: Inhibition of albumin denaturation by Se-Gc

The inhibition of albumin denaturation by selenium nanoparticles synthesized using *Andrographis paniculata* (Se-Gc) followed a concentration-dependent trend, with higher concentrations exhibiting greater inhibition. At 500 µg/ml, Se-Gc showed a mean inhibition of 35.92%, which was slightly lower than the standard anti-inflammatory drug (40.01%). As the concentration decreased, the inhibition percentage gradually declined, with 250 µg/ml, 100 µg/ml, 50 µg/ml, and 10 µg/ml showing inhibition percentages of 31.13%, 30.00%, 28.39%, and 18.36%, respectively. The standard anti-inflammatory compound exhibited the highest inhibition (40.01%), confirming its strong efficacy in preventing protein denaturation. Se-Gc nanoparticles at 500 µg/ml displayed notable inhibition, though slightly lower than the standard, indicating moderate anti-inflammatory potential. Even at lower concentrations, Se-Gc retained a significant inhibitory effect, suggesting its ability to reduce protein denaturation-induced inflammation.

Table 9: IC50 Value of *Andrographis paniculata* (55.28 µg/ml)

log(inhibitor) vs. normalized response - - Variable slope	
Best-fit values	
LogIC50	1.743
HillSlope	-1.209

IC50		55.28
Std. Error		
LogIC50		0.07485
HillSlope		0.2486
95% Confidence Intervals		
LogIC50		1.581 to 1.904
HillSlope		-1.746 to -0.6719
IC50		38.09 to 80.21
Goodness of Fit		
Degrees of Freedom		13
R square		0.8747
Absolute Sum of Squares		2130
Sy.x		12.80
Number of points		
Analyzed	3	15

The anti-inflammatory activity of selenium nanoparticles synthesized using *Andrographis paniculata* (Se-Ap) was evaluated using the albumin denaturation assay. The IC_{50} value, representing the concentration required to inhibit 50% of albumin denaturation, was determined to be 55.28 µg/ml, confirming the reliability of the results (Table 9). These findings suggest that Se-Ap nanoparticles exhibit significant anti-inflammatory activity by inhibiting protein denaturation, a key mechanism involved in inflammation.

These results highlight the promising anti-inflammatory properties of Se-Gc nanoparticles, particularly at higher concentrations, where their inhibition potential is close to that of the standard drug, supporting their potential application as anti-inflammatory agents.

Zinc – *Andrographis paniculata*

Zinc nanoparticles synthesized using *Andrographis paniculata* (Zn-Gc) in the albumin denaturation assay was evaluated.

Table 10: OD Value at 660 nm of Zinc – *Andrographis paniculata* (Zn-Gc)

S. No	Tested sample concentration (µg/ml)	OD Value at 660 nm (in triplicates)			Mean OD Value
1.	Control	1.798	1.801	1.834	1.811
2.	500 µg/ml	1.499	1.510	1.521	1.510
3.	250 µg/ml	1.536	1.525	1.532	1.531

4.	100 µg/ml	1.590	1.544	1.605	1.580
5.	50 µg/ml	1.606	1.636	1.681	1.641
6.	10 µg/ml	1.721	1.784	1.724	1.743
7.	Standard	1.198	1.102	1.178	1.159

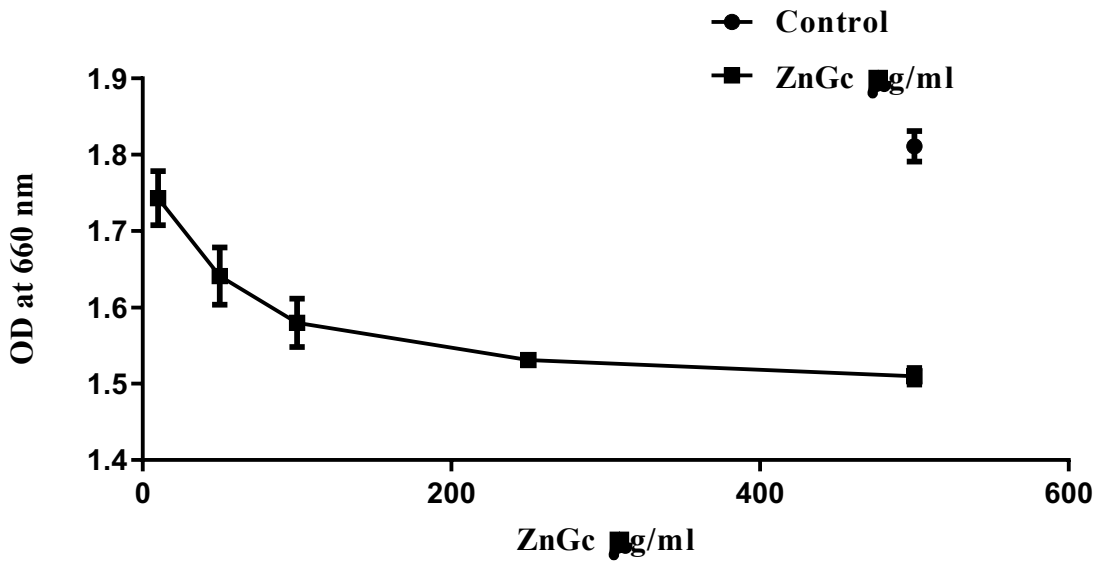

Figure 13: Line graph of Zn-Gc

The optical density (OD) values at 660 nm for zinc nanoparticles synthesized using *Andrographis paniculata* (Zn-Gc) were recorded to assess their effect on albumin denaturation. The control OD value (mean: 1.811) represents complete protein denaturation, while the standard drug (OD range: 1.102–1.198) demonstrated strong inhibition. Zn-Gc nanoparticles at 500 µg/ml showed a reduction in OD values (1.499–1.521), indicating significant inhibition of denaturation. As the concentration decreased, OD values gradually increased, signifying a dose-dependent reduction in anti-inflammatory potential. At the lowest concentration (10 µg/ml), OD values (1.721–1.784) were close to the control, suggesting minimal inhibition (Figure 13). These results indicate that Zn-Gc nanoparticles exhibit moderate anti-inflammatory activity, with higher concentrations showing greater effectiveness in preventing albumin denaturation.

Table 11: Inhibition percentage of albumin denaturation (%) of Zn-Gc

S. No	Tested sample concentration (µg/ml)	Inhibition percentage albumin denaturation (%) (in triplicates)			Mean Value (%)
1.	500 µg/ml	17.2281	16.6207	16.0133	16.6207

2.	250 µg/ml	15.185	15.7924	15.4059	15.4611
3.	100 µg/ml	12.2032	14.7432	11.3749	12.7738
4.	50 µg/ml	11.3197	9.66317	7.17835	9.38708
5.	10 µg/ml	4.96963	1.49089	4.80398	3.75483
6.	Standard	33.8487	39.1496	34.9531	35.9838

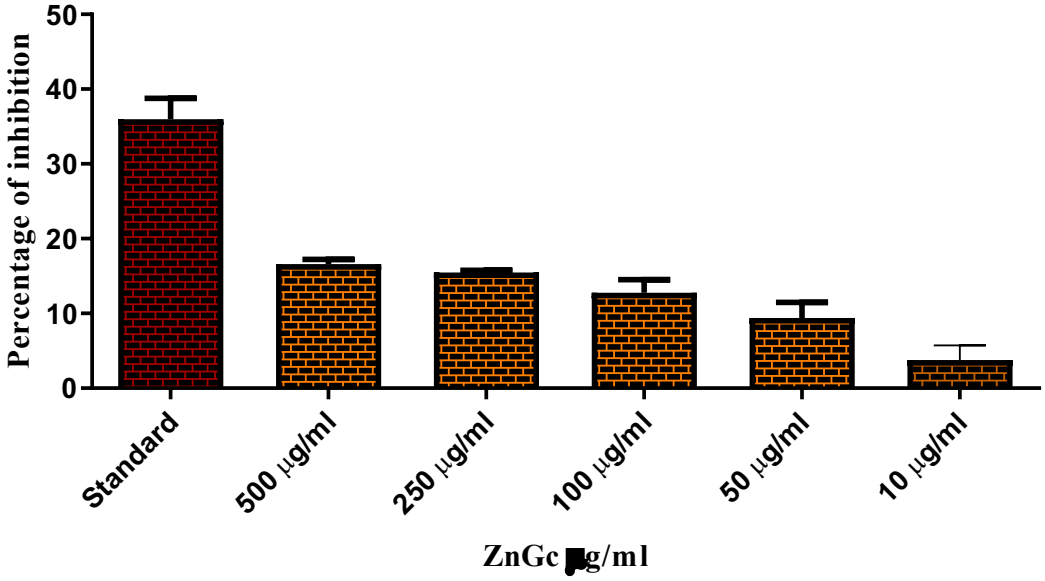

Figure 14: Inhibition of albumin denaturation by Zn-Gc

The inhibition of albumin denaturation by Zn-Gc nanoparticles (*Andrographis paniculata*) followed a dose-dependent pattern, with higher concentrations exhibiting greater inhibition. At 500 µg/ml, Zn-Gc showed a mean inhibition of 16.62%, which was lower compared to the standard anti-inflammatory drug (35.98%). As the concentration decreased, inhibition also gradually declined, with 250 µg/ml, 100 µg/ml, 50 µg/ml, and 10 µg/ml showing inhibition percentages of 15.46%, 12.77%, 9.38%, and 3.75%, respectively (Table).

The standard compound exhibited the highest inhibition (35.98%). Zn-Gc nanoparticles at 500 µg/ml displayed moderate inhibition but were significantly lower than the standard, indicating a weaker anti-inflammatory potential. At lower concentrations, Zn-Gc showed minimal inhibition, suggesting limited effectiveness in preventing protein denaturation-induced inflammation.

Table 12: IC50 Value of Zinc – *Andrographis paniculata* 60.06 µg/ml

log(inhibitor) vs. normalized response -- Variable slope		
Best-fit values		
LogIC50		1.779
HillSlope		-1.782
IC50		60.06
Std. Error		
LogIC50		0.04800
HillSlope		0.3798
95% Confidence Intervals		
LogIC50		1.675 to 1.882
HillSlope		-2.602 to -0.9615
IC50		47.30 to 76.25
Goodness of Fit		
Degrees of Freedom		13
R square		0.9283
Absolute Sum of Squares		1503
Sy.x		10.75
Number of points		
Analyzed	3	15

The anti-inflammatory potential of zinc nanoparticles synthesized using *Andrographis paniculata* (ZnAp) was evaluated through the albumin denaturation assay. The IC_{50} value, which represents the concentration required to inhibit 50% of albumin denaturation, was determined to be 60.06 µg/ml, confirming the reliability of the results. These findings suggest that ZnAp nanoparticles exhibit significant anti-inflammatory activity by effectively inhibiting protein denaturation, a critical process implicated in inflammation.

These findings indicate that Zn-Gc nanoparticles exhibit mild anti-inflammatory properties, with their inhibition potential being notably lower than the standard drug. While they show some anti-inflammatory activity at higher concentrations, their effectiveness in therapeutic applications may be limited compared to other zinc nanoparticle formulations.

CONCLUSION

Based on the anti-inflammatory results of selenium and zinc oxide nanoparticles synthesized using *Andrographis paniculata*, it was observed that selenium nanoparticles (Se-Ap) exhibited stronger anti-inflammatory activity compared to zinc nanoparticles (Zn-Ap). At the highest tested concentration of

500 µg/ml, Se-Ap showed a maximum inhibition of 75.41%, whereas Zn-Ap exhibited a comparatively lower inhibition of 68.49%. This trend of higher activity for selenium nanoparticles was consistent across all tested concentrations, indicating a better dose-dependent anti-inflammatory response. The results suggest that selenium nanoparticles synthesized using *Andrographis paniculata* have greater potential for anti-inflammatory applications than the corresponding zinc oxide nanoparticles.

REFERENCES

Aden, D. P., Fogel, A., Plotkin, S., Damjanov, I., & Knowles, B. B. (1979). Controlled synthesis of HBsAg in a differentiated human liver carcinoma-derived cell line. Nature, 282(5739), 615-616.

Chandrasekaran, C. V., Gupta, A., & Agarwal, A. (2010). Effect of an extract of Andrographis paniculata leaves on inflammatory and allergic mediators in vitro. *Journal of ethnopharmacology*, *129*(2), 203-207.

E.Z. Gomaa, Microbial mediated synthesis of zinc oxide nanoparticles, characterization and multifaceted applications, J. Inorg. Organomet. Polym. Mater. 32 (11) (2022) 4114–4132.

Hussain, I., Singh, N. B., Singh, A., Singh, H., & Singh, S. C. (2016). Green synthesis of nanoparticles and its potential application. *Biotechnology letters*, *38*, 545-560.

Keservani, R. K., & Sharma, A. K. (Eds.). (2018). *Nanoconjugate nanocarriers for drug delivery*. CRC Press.

Kharissova OV, Dias HR, Kharisov BI, Pérez BO, Pérez VM. The greener synthesis of nanoparticles. Trends Biotechnology 2013;31(4):240–8.

Kwak, B., Ozcelikkale, A., Shin, C. S., Park, K., & Han, B. (2014). Simulation of complex transport of nanoparticles around a tumor using tumor-microenvironment-on-chip. *Journal of Controlled Release*, *194*, 157-167.

Mehnath, S., Das, A. K., Verma, S. K., & Jeyaraj, M. (2021). Biosynthesized/green-synthesized nanomaterials as potential vehicles for delivery of antibiotics/drugs. In *Comprehensive analytical chemistry* (Vol. 94, pp. 363-432). Elsevier.

Mishra, S. K., Sangwan, N. S., & Sangwan, R. S. (2007). Phcog rev.: Plant review Andrographis paniculata (Kalmegh): A review. *Pharmacognosy Reviews*, *1*(2), 283-298.

Noruzi, M. (2015). Biosynthesis of gold nanoparticles using plant extracts. *Bioprocess and biosystems engineering*, *38*(1), 1-14.

Singh, P., Kim, Y. J., Zhang, D., & Yang, D. C. (2016). Biological synthesis of nanoparticles from plants and microorganisms. *Trends in biotechnology*, *34*(7), 588-599.

Thermo Fisher Scientific, USA

Traded Medicinal Plants Database.

Tran, P. A., & Webster, T. J. (2011). Selenium nanoparticles inhibit Staphylococcus aureus growth. *International journal of nanomedicine*, 1553-1558.

W.C.W. Chan, B.Y.S. Kim, J.T. Rutka, review article, N. Engl. J. Med. (2010)